MICROSTRUCTURE AND MECHANICAL PROPERTIES OF $MoSi_2$ - BASES COMPOSITES

B. Ballóková, P. Hvizdoš, M. Besterci, M. Zumdick, A. Böhm

Abstract

The purpose of the present investigation was to explore microstructure and mechanical properties of composite materials with different amounts of secondary phase (SiC, nano SiC, Si_3N_4), and their comparison with monolithic $MoSi_2$. The main criteria for the assessment of mechanical properties were hardness, mechanical strength, and fracture toughness determined by two different methods. The results showed that composite materials with 10% nano SiC particles had the best mechanical properties compared to all other studied materials. The creep resistance of $MoSi_2$ composite materials in ambient atmosphere was studied in the temperature range 1000 – 1400°C under a load of 100 MPa.

Keywords: composite material, fracture toughness, mechanical properties, microstructure, creep behaviour

INTRODUCTION

Molybdenum disilicide based materials are candidate materials for high temperature structural applications as furnace heating elements and electrical conductors in silicon intergrated circuit design, or parts of engines [1]. The $MoSi_2$ phase is a borderline ceramic-intermetallic compound with both covalent and metallic atomic bonds. Besides traditional use as heating elements, materials based on $MoSi_2$ appear to be promising candidates for a wide variety of high temperature structural applications where high stress and temperature durability is required [2-4]. The reasons for that are the attractive properties of $MoSi_2$ such as the high melting point, 2030°C, excellent oxidation and corrosion resistance, thermodynamical stability, high temperature ductility above the brittle-to-ductile transition temperature close to 1000°C, good electrical conductivity, machinability, and a relatively low cost as well. The main disadvantage of $MoSi_2$ is the low fracture toughness and low strength at temperatures below 1000°C, and low creep resistance at high temperatures. Several ways of improving the performance of $MoSi_2$ based composites have been developed by incorporating SiC, Si_3N_4 and SiC nano particles or SiC whiskers into the matrix [4-8]. During the last decade a number of papers have been aimed at the study of creep behaviour of $MoSi_2$ based materials, mainly in compression and tensile loading mode [9-12].

The aim of this work was to investigate the microstructure, mechanical properties - hardness, fracture toughness, bending strength in air at room temperature, and the creep resistance of the $MoSi_2$ - 10% SiC, $MoSi_2$ - 15% SiC, $MoSi_2$ - 10% nano SiC and $MoSi_2$ - 10% Si_3N_4 materials in air at temperatures up to 1400°C.

Beáta Ballóková, Michal Besterci, Institute of Materials Research, Slovak Academy of Sciences, Košice, Slovak Republic
Pavol Hvizdoš, Department of Materials Science and Metallurgical, Engineering Polytechnic University of Catalonia, Barcelona, Spain
Marcus Zumdick, Alexander Böhm, Fraunhofer Institute for Applied Materials Research, Dresden, Germany

EXPERIMENTAL MATERIALS AND METHODS

The composites were prepared by a powder metallurgical technology based on a patented technique [4] using a high energy milling (HEM) process. After milling in a planetary ball mill „Pulverisette 5“ (Fritsch, Germany) the resulting high dispersive powder mixtures exhibit a remarkable sinterability, reaching high densities (>95% theoretical density (TD)) after pressureless sintering at moderate temperatures (1600°C, Ar-atmosphere). To produce the composites, the ceramic particles were added to high energy milled Mo + 2 Si powder mixtures with a subsequent homogenization of the mixture in the ball mill. To avoid impurities, namely oxygen and iron (abrasion from the milling balls), the containers of the planetary ball mill were filled under a protective atmosphere (Ar4.8, glove-box). To get samples for the investigations the milled powders were densified by hot pressing (35 MPa, 1550°C) under an inert argon atmosphere.

$MoSi_2$ based materials were supplied in the form of disks with diameters of 50 mm and a thickness of 5 mm. The disks were cut to obtain the bending bars with dimensions of 3 mm x 4 mm x 42 mm. For measurement of the hardness at room temperature, the indentation of a polished surface by Vickers pyramid was used. The indentation load *(P)* was 148 N.

The fracture toughness (K_{IC}) was measured by means of methods, i.e. indentation fractures (IF) and indentation strength (IS), using Vickers indents. In the IF method, the K_{IC} was calculated using Shetty's formula.

$$K_{IC} = 0.0889.\left(HV \cdot P/4 \cdot l\right)^{0.5} \quad (1)$$

where l = c - a, c being the indentation crack length measured on surface from the centre of the indentation imprint to the crack tip, a is the half-diagonal length of the indentation impression. In the IS method, the indented specimens were broken in four-point bending and the fracture toughness was calculated as

$$K_{IC} = 0.88 \cdot \left(\sigma_f \cdot P^{1/3}\right)^{1/4} \quad (2)$$

where σ_f is the fracture stress.

The strength tests were carried out in ambient air at room temperature using a standard testing machine Instron 1362 with four-point flexure jig of inner/outer roller spans of 20/40 mm, respectively. The tensile surfaces of the used samples were polished, in order to avoid fracture initiation from machining flaws. The microstructure of the materials was studied using light microscopy and scanning electron microscopy (SEM). Polarized light was used for microstructure observation.

The creep tests were carried out in four-point bending in air using 11/22 mm fixture. The samples, loaded statically by a dead-weight system at a constant stress of 100 MPa, were tested at 1000 – 1400°C. From the measured deflection of the middle of the sample, the outer fibre strain was calculated and the strain-time (ε - t) profiles were recorded. The experimental setting allows one to measure deflections up to 1 mm, which limited possible bending strain that could be properly detected to 1%. Assuming Arrhenian temperature dependence of the stationary creep rate:

$$\dot{\varepsilon} = const.\sigma^n \exp\left(\frac{Q_A}{RT}\right),$$

where R is the gas constant, T the temperature in Kelvin, σ the applied stress, n the stress exponent, the apparent activation energies Q_A for both materials at stress of 100 MPa were calculated from the strain rate vs. 1/T plots.

RESULTS AND DISCUSSION

Examples of microstructures of the studied materials are shown in Fig.1 and 2 at low magnification.

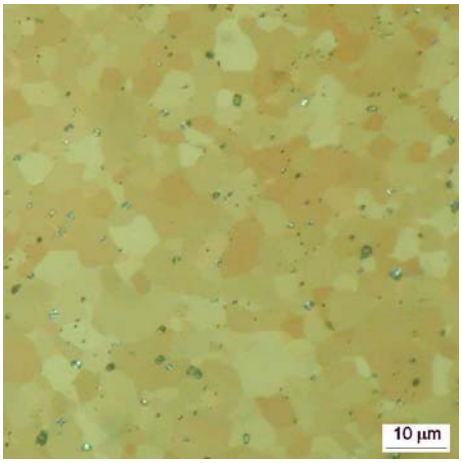

Fig.1. Characteristic microstructure of the monolithic $MoSi_2$.

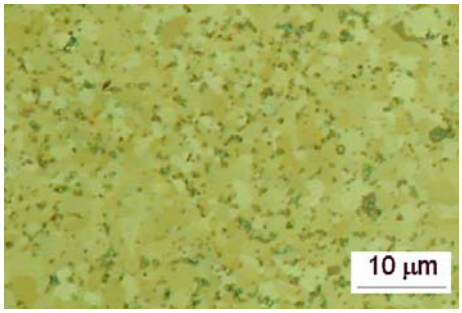

Fig.2. Characteristic microstructure of the $MoSi_2$+ 10% nano SiC.

Figure 1 shows pure material $MoSi_2$ in cross-polarized illumination. The average grain size was approx. 5 μm. The microstructure contains pores with sizes from 0.1 to 3 μm. Using an EDX analyzer, three phases were identified: $MoSi_2$ matrix grains, amorphous SiO_2 and Mo_5Si_3 (so-called hexagonal Nowotny phase).

Figure 2 shows material $MoSi_2$-10% nano SiC. The microstructures were heterogeneous, the secondary phase was uniformly distributed. It has to be noted that in all cases the introduction of the dispersoid particles inhibited the growth of the $MoSi_2$ grains. The monolithic material had the largest grains (approx. 10 μm) and fewest defects.

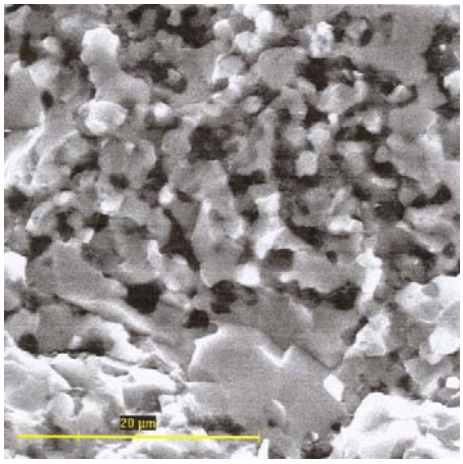

Fig.3. Typical fracture of composite $MoSi_2$+SiC.

A typical fracture of composite material $MoSi_2$ + 10% nano SiC is shown in Fig.3. Fractographic investigation of the fracture origins/strength degrading defects revealed that these are mainly areas with a high content of secondary particles and areas with a higher concentration of pores. The crack propagation in the composites had an intercrystalline character with cleavage facets.

Hardness, mechanical strength, and fracture toughness of monolithic $MoSi_2$ and the composites with different volume fraction of secondary phases are summarized in Tab.1.

Tab.1. Mechanical properties of investigated materials.

Experimental material	HV [GPa]	KIC (IS) [MPa.m$^{1/2}$]	KIC (IF) [MPa.m$^{1/2}$]	σ [MPa]
$MoSi_2$	9.61 ± 0.17	4.13	3.74	233
$MoSi_2$ + 10% SiC	11.15 ± 0.11	5.52	4.91	277
$MoSi_2$ + 15% SiC	10.97 ± 0.17	6.65	4.87	369
$MoSi_2$ + 10% nanoSiC	12.19 ± 0.16	6.15	5.48	402
$MoSi_2$ + 10% Si_3N_4	11.34 ± 0.38	5.83	4.23	325

All mentioned mechanical properties were improved by adding ceramics particles in matrix $MoSi_2$. The most dramatic improvement of the hardness of the monolithic material (9.61 GPa) was achieved in the material with 10% nano SiC particles (max. 12.19 GPa), which agrees with literature data [1,5]. Similarly increased were the values of the fracture toughness. Comparison of the two methods of fracture toughness measurement indicates better sensitivity and reliability of the IS method which is less influenced by the human factor.

The composites with 10% SiC nano particles and 15% SiC particles had the highest values of bending strength at room temperature, 402 MPa and 369 MPa, respectively. By comparing these results, it can be seen that more homogeneous distribution of smaller (nano) particles in the bulk positively influences the properties of the composites at room temperature, mainly the strength, because it prevents the formation of large defects.

The results of the creep tests are illustrated in Figs.4-6. The figures show the creep curves for experimental materials in the whole temperature range.

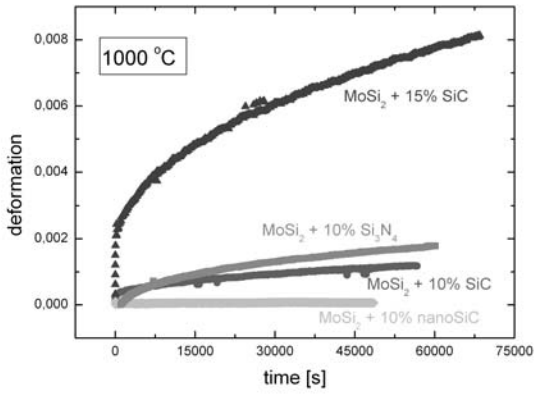

Fig.4. Creep curves for studied composite materials (stress 100 MPa, temperature 1000°C).

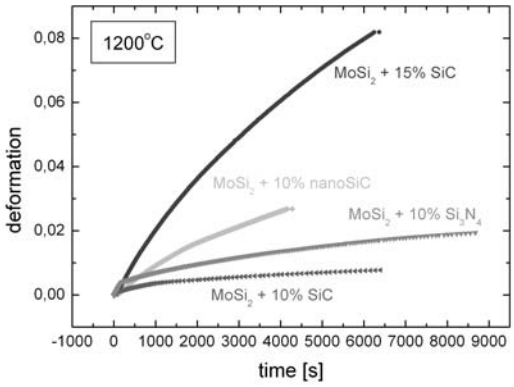

Fig.5. Creep curves for studied composite materials (stress 100 MPa, temperature 1200°C).

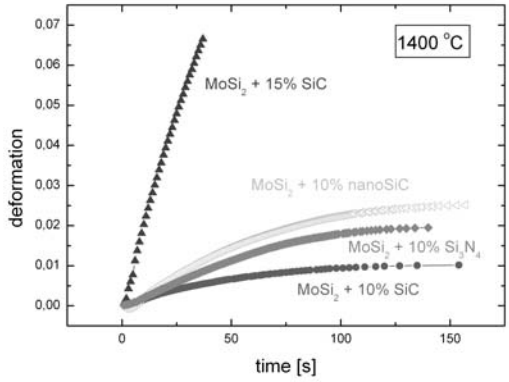

Fig.6. Creep curves for studied composite materials (stress 100 MPa, temperature 1400°C).

At lower temperatures (1000°C, 1100°C) the performance of $MoSi_2$-10% nano SiC was about one order of magnitude better than that of the other composites.

Overall comparison of the creep behaviour of the composites (temperatures 1000 to 1400°C) shows that the material with 10% nano SiC particles exhibited a significant decrease of creep resistance with increasing temperature. At 1200 and 1400°C, similarly as at 1000°C, the material containing 15% SiC particles was the least creep resistant one. The material with 10% SiC particles retained the highest creep resistance.

Tertiary creep was reached in no experiment, and moreover, it was not always possible to determine the stationary creep exactly in the experimental arrangement used. In such cases the minimum values of the strain rate, calculated from the final (usually nearly straight) part of the creep curve, and were taken as the "steady-state" strain rates. Nevertheless, the obtained results were consistent and they are mutually comparable. The values of the apparent activation energy are given in Table 5 and lie between 303 and 424 kJ/mol. The results for the monolithic material obtained earlier by the same experimental method gave the value of Q_A= 244 kJ/mol.

Tab.5. The apparent activation energies of the investigated materials (Q_A) in kJ/mol.

$MoSi_2$	$MoSi_2$ + 10% SiC	$MoSi_2$ + 15% SiC	$MoSi_2$ + 10% Si_3N_4	$MoSi_2$ + 10% nano SiC
244	351	391	342	424

CONCLUSION

On the basis of the present study, the followed conclusions can be proposed:

- The material $MoSi_2$ containing 10% nano SiC particles had the optimum microstructue.
- The combination of the mechanical properties (*HV*, K_{IC}, σ) at room temperature indicates the best characteristics of the $MoSi_2$ with 10% nano SiC particles.
- Creep tests of the investigated composite materials confirmed their relatively good creep resistance. Creep parameters changed with temperature differently in each material. The highest creep resistance, at temperature 1000°C, had the material $MoSi_2$-10% nano SiC. At the temperature interval 1200 - 1400°C the materials $MoSi_2$ - 10% SiC particles and $MoSi_2$ - 10% Si_3N_4 particles were the most resistant.
- The values of the apparent activation energies of the composites were between 350-425 kJ/mol, in contrast to 244 kJ/mol or 250 kJ/mol [14] for the monolithic system.

Acknowledgement

This work was supported by the Slovak Grant Agency of the Ministry of Education of the Slovak Republic and the Slovak Academy of Sciences, Project. No.2/5142/25.

REFERENCES

[1] PETROVIC, JJ., HONNELL, RE., MITCHELL, TE.: Ceram. Eng. Sci. Proc., vol. 12, 1991, p. 1633
[2] SHAW, L., MIRACLE, D., ABBASCHIAN, R.: Acta Metal. Mater., vol. 43, 1995, p. 4267
[3] COSTA E SILVA, A., KAUFMAN, MJ.: Mater. Sci. Eng. A, vol. 195, 1995, p. 75
[4] SCHOLL, R., BÖHM, A., KIEBACK, B.: Material Science and Engineering A, vol. 261, 1999, p. 204
[5] MALOY, S., HEUER, AH., LEWANDOWSKI, J., PETROVIC, JJ.: J. Amer. Ceram. Soc., vol. 74, 1991, p. 2704
[6] JAYASHANKAR, S., KAUFMAN, MJ.: Scripta Met. Mater., vol. 26, 1992, p. 1245
[7] YAMADA, T., HIROTA, K., YAMAGUCHI, O., ASAI, J., MAKARAYAMA, Y.: Mater. Res. Bulletin, vol. 7, 1995, p. 851
[8] BHATTACHARYA, AK., PETROVIC, JJ.: J. Amer. Ceram. Soc., vol. 75, 1992, p. 23
[9] SOBOYEJO, W., BROOKS, D., CHEN, LC.: J. Amer. Ceram. Soc., vol. 78, 1995, p. 1481
[10] SADANANDA, K., FENG, CR., JONES, H., PETROVIC, JJ.: J. Mater. Sci. and Eng. A, vol. 155, 1992, p. 227
[11] SADANANDA, K., FENG, CR.: Mater. Sci. & Eng. A, vol. 170, 1993, p. 199
[12] FRENCH, JD., WIEDERHOM, SM., PETROVIC, JJ. In: Ceramic Engineering & Science Proc., Amer. Ceram. Soc., 1995, p. 129
[13] KOFSTAD, P.: High Temperature Oxidation of Metals. New York : Wiley, 1966